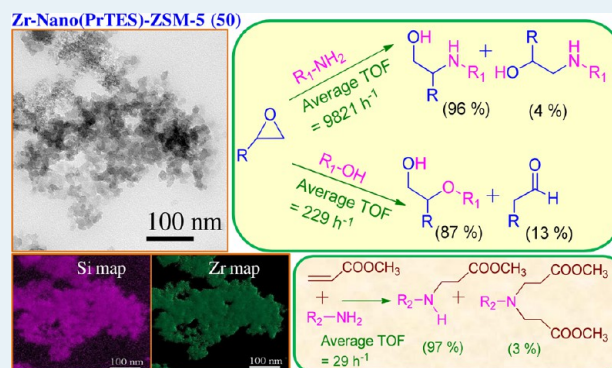


Highly Efficient Nanocrystalline Zirconosilicate Catalysts for the Aminolysis, Alcoholysis, and Hydroamination Reactions

Rajkumar Kore,[†] Rajendra Srivastava,^{*,†} and Biswarup Satpati[‡][†]Department of Chemistry, Indian Institute of Technology Ropar, Rupnagar-140001, India[‡]Saha Institute of Nuclear Physics, 1/AF, Bidhannagar, Kolkata 700 064, India**S** Supporting Information

ABSTRACT: Nanocrystalline zirconosilicates and titanosilicates with MFI framework structure were hydrothermally synthesized by the addition of organosilanes in the synthesis composition of conventional zirconosilicate and titanosilicate materials. Materials were characterized by a complementary combination of X-ray diffraction, nitrogen sorption, scanning/transmission electron microscopy (S/TEM), ammonia temperature-programmed desorption (TPD), Fourier transform infrared (FT-IR) spectroscopy, and ultraviolet–visible (UV-vis) spectroscopic investigations. Nanocrystalline zeolite catalysts of the present study are reusable. They exhibit significantly higher catalytic activities in aminolysis and alcoholysis compared with the hitherto known catalysts. A range of β -amino alcohols/ β -alkoxy alcohols with high regioselectivity were synthesized using zirconosilicates. Application of these materials was also extended in the synthesis of aminoesters by the hydroamination reaction of methyl acrylates and amines. Structure activity relationship was explained based on acidity measurements, reactivity of amines/alcohols, and adsorption of reactants on catalysts.

KEYWORDS: nanocrystalline zeolite, zirconosilicate, titanosilicate, ring-opening of epoxide, hydroamination, β -amino alcohols, amino acid derivatives



1. INTRODUCTION

The heterogeneous catalyst plays a very important role in bulk chemical industries, especially in the petrochemical industry.¹ Fine chemicals and pharmaceuticals are conventionally synthesized using homogeneous catalysts.² But, it can also be synthesized using heterogeneous catalysts. Heterogeneous catalysts can easily be separated from the reaction mixture by simple filtration and recycled, which makes the process eco-friendly and less expensive.³ Heterogeneous catalysts can be successively developed by tailoring the physicochemical properties of zeolites, clays, and metal oxides.⁴ Among these materials, zeolites have been given more attention, because of their acidic properties, shape selectivity, and isomorphous substitution of transition-metal ions to incorporate redox properties.^{4a,5} However, when large reactants are involved, many of these materials exhibit several limitations, especially in the synthesis of fine chemicals. To overcome this problem, initially noncrystalline mesoporous aluminosilicates were developed.⁶ However, their activity was found to be much lower than the activity of crystalline microporous aluminosilicate in the reaction requiring strong acidity.^{7,8} Recently, attempts were made to prepare nanocrystalline aluminosilicate of different framework structure, which possess intercrystalline/intracrystalline mesopores.⁷ Nanocrystalline materials with mesopores were prepared using soft (ionic/nonionic/neutral/

polymeric templates) and hard templates.^{7,8} Nanocrystalline materials with mesopores exhibited significantly high activity than conventional microporous materials. Furthermore, nanocrystalline materials with mesopores exhibited improved retardation against deactivation during catalytic investigation.⁹ Most of these studies were based on nanocrystalline aluminosilicates. There are few reports where transition-metal-containing nanocrystalline materials with mesopores were prepared and used in catalytic investigations.¹⁰ Our research group has also contributed in this area and reported the synthesis and applications of nanocrystalline materials with mesopores with MFI and Beta framework structures.¹¹ In this study, we report the synthesis of nanocrystalline zirconosilicates and titanosilicates with MFI framework structure. Very recently, synthesis and applications of Fe and Ti containing nanocrystalline materials have been reported.^{10b,12} Synthesis of multimodal Zr-Silicalite-1 zeolite nanocrystal and mesoporous zirconosilicate has also been reported recently.¹³

Amines, alcohols, and amino alcohols are significantly important synthetic intermediates.¹⁴ A variety of important organic compounds can be obtained from these synthetic

Received: August 26, 2013

Revised: October 29, 2013

Published: October 30, 2013

intermediates. Therefore, eco-friendly synthesis of amines, alcohols, and amino alcohols are of great interest to catalysis researchers. Several synthesis methods are known for their synthesis. Ring-opening of epoxides with amines/alcohols leads to the formation of amino alcohols/alkoxy alcohols. Epoxides are the three-membered heterocyclic ring, which are more reactive than ethers due to ring strain. Nucleophiles attack the electrophilic C of the C–O bond causing it to break and thereby resulting in ring-opening. It is susceptible to attack by a range of nucleophiles, including nitrogen (e.g., ammonia, amines, azides), oxygen (e.g., water, alcohols, phenols, acids), and sulfur (thiol)-containing compounds, leading to bifunctional molecules of great industrial value. For example, β -amino alcohols are used in the synthesis of β -blockers, insecticidal agents, and oxazolines.¹⁴ β -alkoxy alcohols are obtained by the ring-opening reaction of epoxides with alcohols. β -alkoxy alcohols are used as intermediates for the synthesis of several pharmaceutical compounds such as antitumorals or immune-suppressives.¹⁵ Hydroamination is one of the well-known atom economical method to produce substituted amines.¹⁵ Hydroamination is the addition of an N–H bond of an amine across C=C or C≡C bonds of an alkene or alkyne.¹⁶ Hydroamination of activated olefin with amine is a simple approach to synthesize amino acid derivatives.¹⁷

Ring-opening of epoxides and hydroamination reactions are catalyzed by acid or base catalysts. Several homogeneous acid catalysts such as metal halides, metal triflates, ionic liquids, and sulfamic acid have been reported to catalyze these transformations.¹⁸ However, many of these methods suffer from several disadvantages such as poor regioselectivity, long reaction time, high temperature, use of stoichiometric amount of catalyst, and the use of expensive reagents or catalysts. Hence, there is need to develop more efficient and reusable solid acid catalysts that are active at low temperatures and avoid the use of solvent. Solid acid catalysts such as zeolites and amorphous mesoporous materials have been reported.¹⁹ Very recently, amorphous mesoporous titanasilicates and microporous TS-1 have been reported for the ring-opening of epoxides.²⁰ Efforts were also made to prepare nanocrystalline titanasilicates and demonstrated their applications in the epoxidation and hydroxylation reactions.^{12a,c,d}

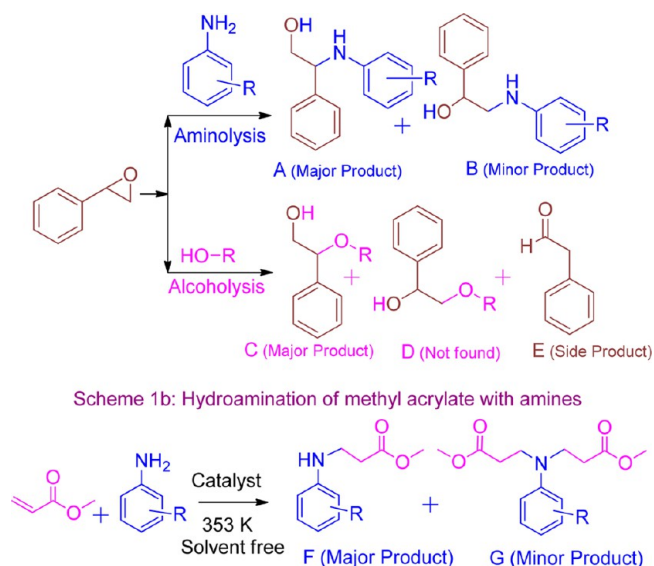
In this manuscript, nanocrystalline zirconosilicates and titanasilicates were synthesized and their application in the ring-opening of epoxide with amines and alcohols (Scheme 1a) were investigated. Application of these materials was also extended in the hydroamination of methyl acrylate with amines (Scheme 1b). For comparative studies, microporous zirconosilicate and titanasilicate were also prepared. To the best of our knowledge, this is the first report that involves the exceptionally high catalytic activity of nanocrystalline zirconosilicate compared with the hitherto known catalysts in the ring-opening of epoxides with amines/alcohols.

2. EXPERIMENTAL SECTION

2.1. Material Preparation. In this study, nanocrystalline ZSM-5 materials were synthesized in the presence of a small amount (7% or 10%, with respect to the silica source) of additive such as propyl triethoxy silane (hereafter referred as PrTES) or [(C₂H₅O)₃SiC₃H₆N(CH₃)₂C₁₆H₃₃Cl] (hereafter referred as TPHAC) in order to disfavor microcrystalline (bulk) zeolite formation.

Ti containing nanocrystalline ZSM-5 materials were prepared by following the molar composition of 0.9 TEOS/0.1 PrTES or 0.1TPHAC/*x* TBOT/0.3 TPAOH/30 H₂O, whereas Zr-containing nanocrystalline ZSM-5 materials were prepared by following the molar

Scheme 1. (a) Ring-Opening of Epoxide with Amines/Alcohols and (b) Hydroamination Reaction of Methyl Acrylate with Amines



composition of 0.93 TEOS/0.07 PrTES or 0.07 TPHAC/*x* ZrIPO/0.35 TPAOH/40 H₂O. Ti/Zr-containing nanocrystalline ZSM-5 prepared with PrTES is represented as Ti/Zr-Nano(PrTES)-ZSM-5 (*y*), whereas Ti/Zr-containing nanocrystalline ZSM-5 prepared with TPHAC is represented as Ti/Zr-Nano(TPHAC)-ZSM-5 (*y*), where *y* represents the Si/M ratio. Detailed synthesis of nanocrystalline titanasilicate/zirconosilicates is provided in the Supporting Information.

Conventional Ti-ZSM-5 (50), Zr-ZSM-5 (50), and Al-ZSM-5 (50) were synthesized using the similar procedure that was adopted for the preparation of nanocrystalline ZSM-5 materials, but in the absence of PrTES/TPHAC.

2.2. Material Characterization and Procedure for Catalytic Reactions. Description about material characterization techniques used in this study, procedure for various liquid phase catalytic reactions reported in this study, and details about average turnover frequency (TOF) are provided in the Supporting Information.

3. RESULTS AND DISCUSSION

3.1. Catalyst Characterization. Powder X-ray diffraction (XRD) patterns of nanocrystalline ZSM-5 samples and conventional ZSM-5 samples were found to be identical and showed the characteristic peaks of crystalline MFI structure (see Figures S1a and S1b in the Supporting Information). After careful examination of the XRD patterns, a shift of peaks toward lower 2θ values was observed for Zr/Ti-incorporated ZSM-5 materials (see Figures S1c and S1d in the Supporting Information). This shift is attributable to the substitutions of Si by larger metal ions (Shannon radii: ²¹ 0.73 Å for Zr⁴⁺, 0.56 Å for Ti⁴⁺, and 0.40 Å for Si⁴⁺), which results in an increase of their cell volume (see Table S1 in the Supporting Information). The N₂-adsorption investigations (see details in the Supporting Information) reveal that the external surface area and pore volume of nanocrystalline ZSM-5 materials are much larger than that of conventional ZSM-5 materials (Table 1). Nanocrystalline ZSM-5 was obtained by the addition of PrTES/TPHAC in the synthesis composition of conventional ZSM-5. PrTES/TPHAC contains only three hydrolyzable moieties with one hydrophobic alkyl group that is unfavorable for the formation of extended tetrahedral SiO₂ linkages. Consequently, the zeolite growth is significantly retarded at

Table 1. Textural Properties of ZSM-5 Samples Synthesized in This Work

material	Si/M ^a		S _{BET} ^b (m ² /g)	Ext. SA (m ² /g)	V _{Total} (mL/g)	total acidity ^c (mmol/g)
	input	output				
Al-ZSM-5 (50)	50	52.4	332	71	0.26	1.34
Zr-ZSM-5 (50)	50	61.5	463	130	0.27	0.77
Zr-Nano(PrTES)-ZSM-5 (50)	50	57.8	565	260	0.55	0.83
Zr-Nano(TPHAC)-ZSM-5 (50)	50	58.3	594	296	0.56	0.85
Ti-ZSM-5 (50)	50	58.6	425	110	0.26	0.60
Ti-Nano(PrTES)-ZSM-5 (50)	50	59.1	603	252	0.60	0.57
Ti-Nano(TPHAC)-ZSM-5 (50)	50	57.6	621	280	0.62	0.59
Zr-Nano(PrTES)-ZSM-5 (50) (recycled catalyst)	50	58.5	542	256	0.51	0.85

^aObtained by ICP analysis. ^bS_{BET} calculated from the adsorption data obtained in the region of 0.05 < P/P₀ ≤ 0.3. ^cObtained by NH₃ TPD analysis.

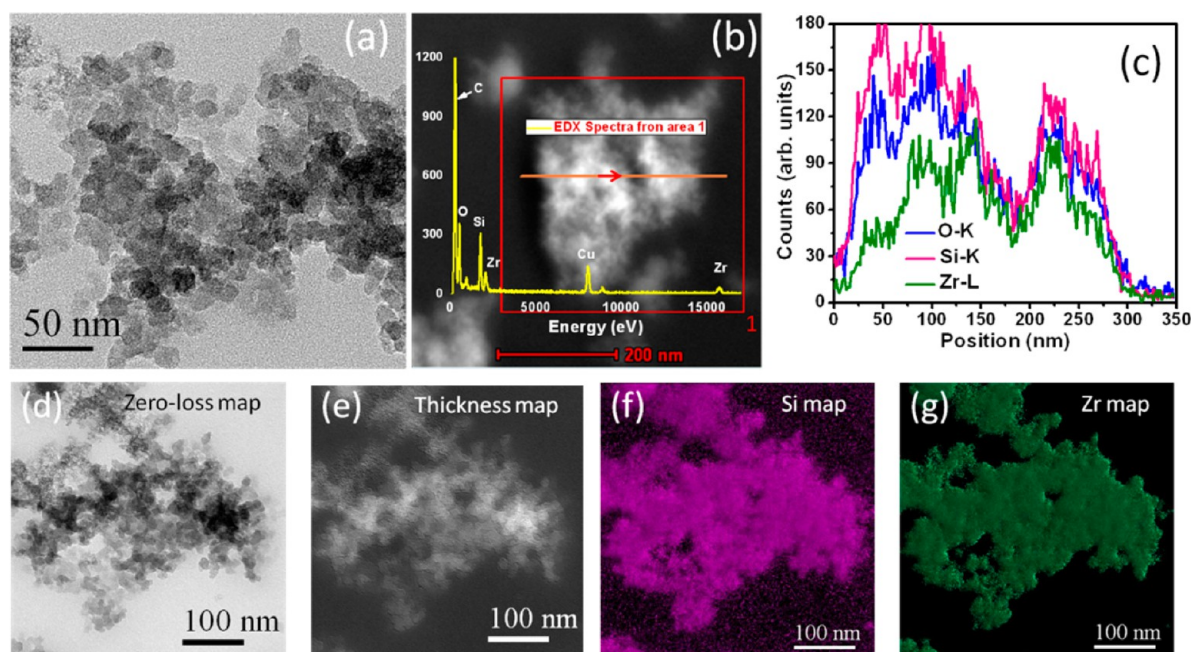


Figure 1. (a) HRTEM image, (b) HAADF images (and, in inset, the EDX spectra from a region marked as “area 1”), and (c) EDX line profile for a line shown in panel (b) of Zr-Nano(PrTES)-ZSM-5 (50). EFTEM images of the sample showing (d) unfiltered image, (e) relative thickness map, (f) chemical map of Si (pink), and (g) chemical map of Zr (green).

the organic and inorganic interfaces, resulting in the formation of nanocrystalline zeolites. Mesopores in nanocrystalline ZSM-5 are formed due to the crystal packing of these nanosized zeolite particles.

SEM investigation was made to confirm the morphology of various materials investigated in this study (see details in the Supporting Information). To obtain further in-depth information, TEM investigation was made for some selected samples. The TEM image of Zr-Nano(PrTES)-ZSM-5 (50) confirmed the irregular aggregated nanoparticle morphology with a particle size of 10–20 nm (see Figures 1a and 1b). Atomic contents in these Zr-Nano(PrTES)-ZSM-5 (50) samples were obtained using energy-dispersive X-ray spectroscopy (EDX), which confirms the presence of O, Si, and Zr atoms (inset of Figure 1b). It may be noted that Cu and C signals observed in the EDX mapping are due to the carbon-coated copper grid used in the analysis. Figure 1c shows the atomic content across the line shown in Figure 1b. For a detailed distribution of atomic contents inside the nanocrystals, elemental mapping of Si and Zr was performed using energy-filtered transmission electron microscopy (EFTEM) imaging (see Figures 1d–g). Energy-filtered images were acquired using a contrast aperture

to reduce chromatic aberrations. Chemical maps from Zr M (180 eV) and Si L (99 eV) edges were obtained using jump-ratio method by acquiring two images (one post-edge and one pre-edge), respectively, to extract the background, with an energy slit of 20 eV for Zr, and 10 eV for Si.

The TEM image of Zr-Nano(TPHAC)-ZSM-5 (50) confirmed the aggregated compressed globular/capsule-like morphology with a particle size of 400 nm (Figure 2a). To investigate the chemical composition of the dots and surrounding matrix, we performed high-angle annular dark-field (HAADF) analysis (Figure 2b). It provides the Z-contrast image, where the intensity of scattered electrons is proportional to the square of the atomic number Z. EDX spectrum from a region marked by area 1 in Figure 2b confirms the presence of O, Zr, and Si atoms (Figure 2c). Comparison of concentrations across the structure was made by EDX line profile. The representative EDX line profile across the line shown in Figure 2b shows the elemental distribution of Si, O, and Zr (Figure 2d).

TEM image of Ti-Nano(PrTES)-ZSM-5 (50) shows the spherical/globular morphology with a particle size of 400–500 nm (Figure 3a), which are built with small zeolite nanocrystals

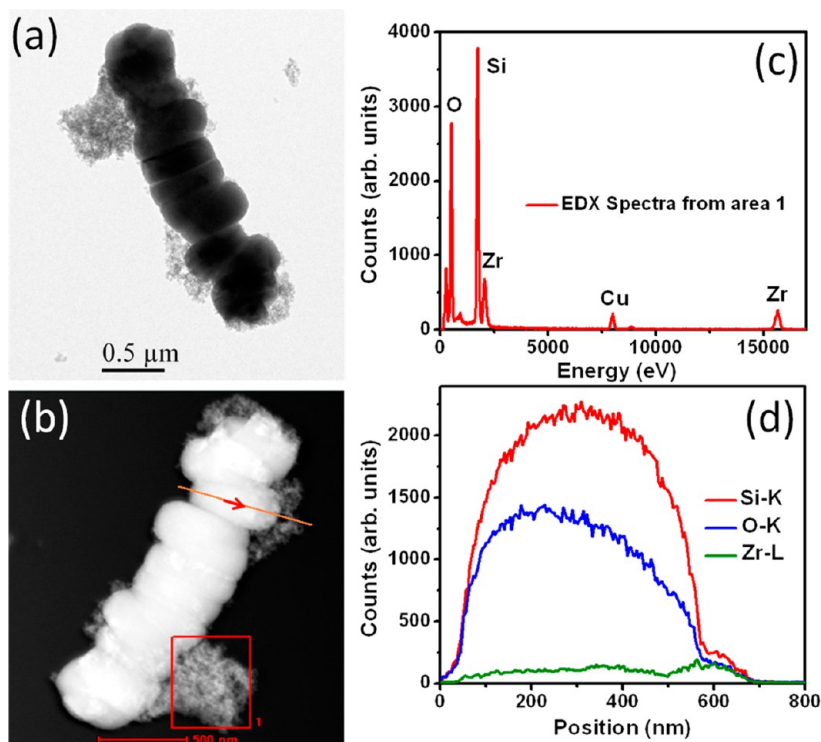


Figure 2. (a) TEM image, (b) HAADF image, (c) EDX spectra of the area highlighted in panel (b), and (d) EDX line profile of the line shown in panel (b) for Zr-Nano(TPHAC)-ZSM-5 (50).

of 10–20 nm (Figure 3b). To investigate the chemical composition of the dots and surrounding matrix, we also performed HAADF analysis in this case (Figure 3c). The EDX spectrum confirms the presence of O, Ti, and Si atoms (figure not shown). Comparison of atomic concentrations across the structure was made by EDX line profile. Figure 3d shows atomic distribution of Si, O, and Ti across the line shown in Figure 3c. For a detailed distribution of Si, O, and Ti, we performed the elemental mapping using EFTEM imaging as illustrated in Figure 3e–h. Energy-filtered images were acquired using a contrast aperture to reduce chromatic aberrations. Chemical maps from Ti M (35 eV) and Si L (99 eV) edges were again obtained using jump-ratio method by acquiring two images (one post-edge and one pre-edge), respectively, to extract the background, with an energy slit of 4 eV for Ti, and 10 eV for Si.

UV–vis and Fourier transform infrared (FT-IR) spectroscopic investigations were made to confirm the incorporation of Ti/Zr in the framework (see details in the Supporting Information).

3.2. Catalytic Activity. **3.2.1. Aminolysis and Alcoholysis Reactions.** The activity of nanocrystalline ZSM-5 materials was investigated in the ring-opening reaction of epoxide with amines and alcohols to form β -amino alcohols and β -alkoxy alcohols, respectively. To optimize the reaction condition for the ring-opening of epoxide with amines, styrene oxide and aniline were chosen as representative epoxide and amine, respectively. Ring-opening of styrene oxide with aniline leads to the formation of two isomerized products A and B (Scheme 1a). Under our reaction conditions, no product was obtained in the absence of catalyst (Table 2). The nature and type of catalyst influenced the epoxide conversion and product A selectivity. If acidity of catalysts is taken into the consideration, then activity of Al-ZSM-5 (50) should be much higher than

that of Zr-ZSM-5 (50)/Ti-ZSM-5 (50). However, ranking of the activity in the case of conventional ZSM-5 materials investigated in this study is found to be

$$\text{Zr-ZSM-5 (50)} > \text{Ti-ZSM-5 (50)} > \text{Al-ZSM-5 (50)}$$

which confirmed that Zr incorporation in the framework is ideally suited for the ring-opening of epoxide. Nanocrystalline ZSM-5 materials exhibited higher catalytic activity than that of conventional ZSM-5 materials. Among the nanocrystalline ZSM-5 materials investigated in this study, Zr-containing nanocrystalline ZSM-5 exhibited the highest catalytic activity. The low activities of conventional ZSM-5 materials are due to their microporous structure. High activities of nanocrystalline ZSM-5 materials can be correlated with their high surface area and intercrystalline mesopores. Large external surface area and mesopores are two important factors that enable better accessibility of the reactant molecules to the active sites and facile diffusion of product molecules through mesopores. Only a marginal increase in the activity of Zr-Nano(PrTES)-ZSM-5 (50) was observed, when compared to Zr-Nano(TPHAC)-ZSM-5 (50). This marginal increase in the catalytic activity of Zr-Nano(PrTES)-ZSM-5 (50) can be correlated to the enhanced accessibility of reactant molecules to the Zr active sites. Based on the catalytic activity, one can conclude that the diffusion of reactants/products is more facile in Zr-Nano(PrTES)-ZSM-5 (50), when compared to Zr-Nano(TPHAC)-ZSM-5 (50).

Influence of reaction parameters such as role of solvent, reaction temperature, amount of catalyst, and Si/Zr ratio was investigated. Reaction parameters were optimized by taking Zr-Nano(PrTES)-ZSM-5 (50) as a catalyst and styrene oxide and aniline as model substrates. Catalytic activity of Zr-Nano(PrTES)-ZSM-5 (50) was found to be higher when reaction was performed in the absence of solvent. Decrease in the

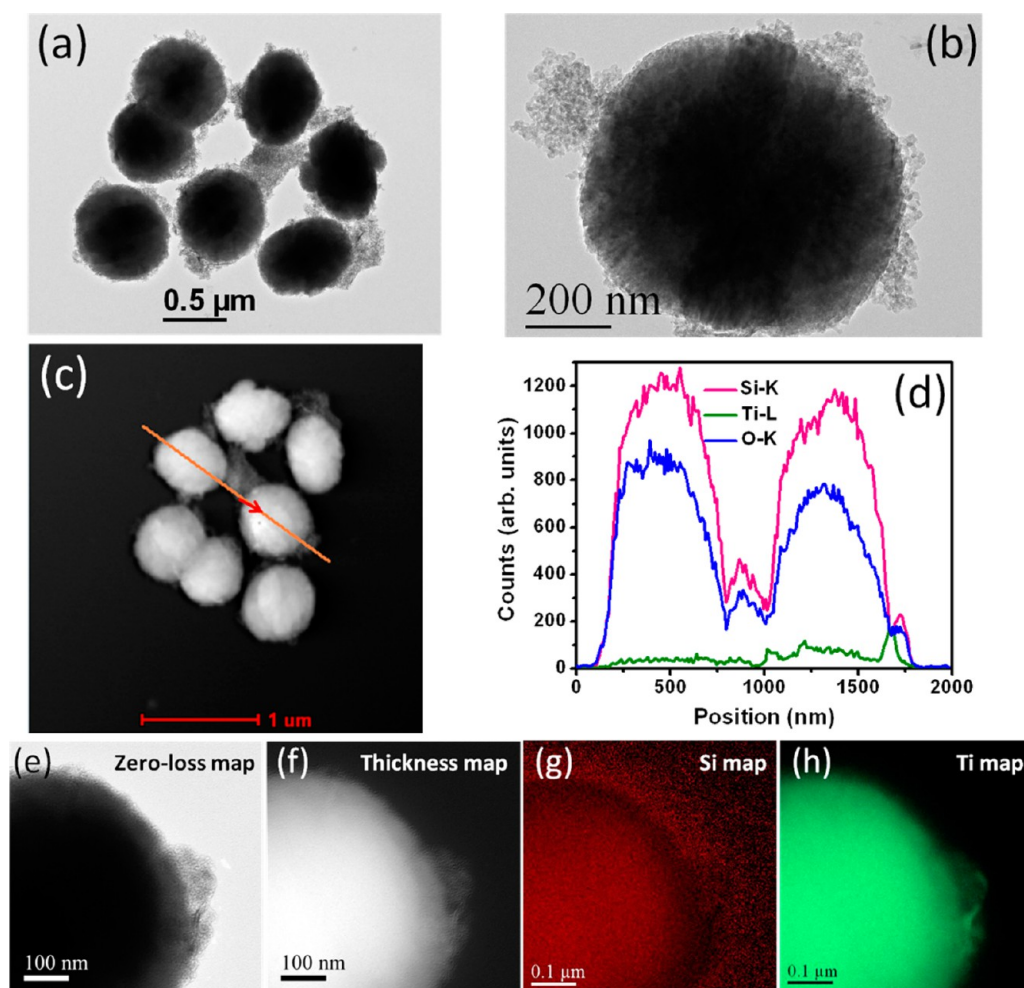


Figure 3. (a and b) TEM image, (c) HAADF image, and (d) EDX line profile of the line shown in panel (c) for Ti-Nano(PrTES)-ZSM-5 (50). EFTEM images of the sample showing (e) unfiltered image, (f) relative thickness map, (g) chemical map of Si (red), and (h) chemical map of Ti (green).

Table 2. Aminolysis of Styrene Oxide with Aniline over Various Zeolite Catalysts^a

entry	catalyst	styrene oxide conversion (%)	product (A/B) selectivity ^b (%)	average TOF ^c (h ⁻¹)
1	none	0		
2	Al-ZSM-5 (50)	trace	trace	
3	Ti-ZSM-5 (50)	1	90/10	84
4	Zr-ZSM-5 (50)	26	96/4	2340
5	Ti-Nano(PrTES)-ZSM-5 (50)	8	92/8	695
6	Ti-Nano(TPHAC)-ZSM-5 (50)	8	91/9	677
7	Zr-Nano(PrTES)-ZSM-5 (30)	93	95/5	5490
8	Zr-Nano(PrTES)-ZSM-5 (50)	83	96/4	7040
9	Zr-Nano(PrTES)-ZSM-5 (100)	62	95/5	9821
10	Zr-Nano(TPHAC)-ZSM-5 (50)	79	94/6	6790

^aReaction conditions: catalyst (25 mg), styrene oxide (5 mmol), aniline (5 mmol), reaction temperature (318 K), reaction time (5 min). ^b[A] = 2-phenyl-2-(phenylamino)ethanol. [B] = 1-phenyl-2-(phenylamino)ethanol. ^cAverage TOF (h⁻¹) = turnover frequency [moles of epoxide converted per mole of active metal (Ti/Zr/Al) per hour].

catalytic activity was observed, when reactions were performed in a solvent medium (see Table S2 in the Supporting Information). Catalytic activity was highly suppressed, when reaction was performed in polar aprotic solvent than nonpolar solvents. This activity difference can be correlated with adsorption of solvent molecule on the catalytic active sites. Epoxide adsorption and activation on active site are key factors for the ring-opening reaction. When no solvent is used, only

reactants molecules are accessible to the active site and high catalytic activity is achieved. Solvent molecules, especially polar solvent molecules can block the active sites due to the competitive adsorption of reactant and solvent molecules. This competitive adsorption creates hindrance for the reactant molecules to reach active sites; therefore, in the presence of solvent, catalytic activity decreased. Influence of temperature on conversion and product selectivity in the aminolysis of styrene

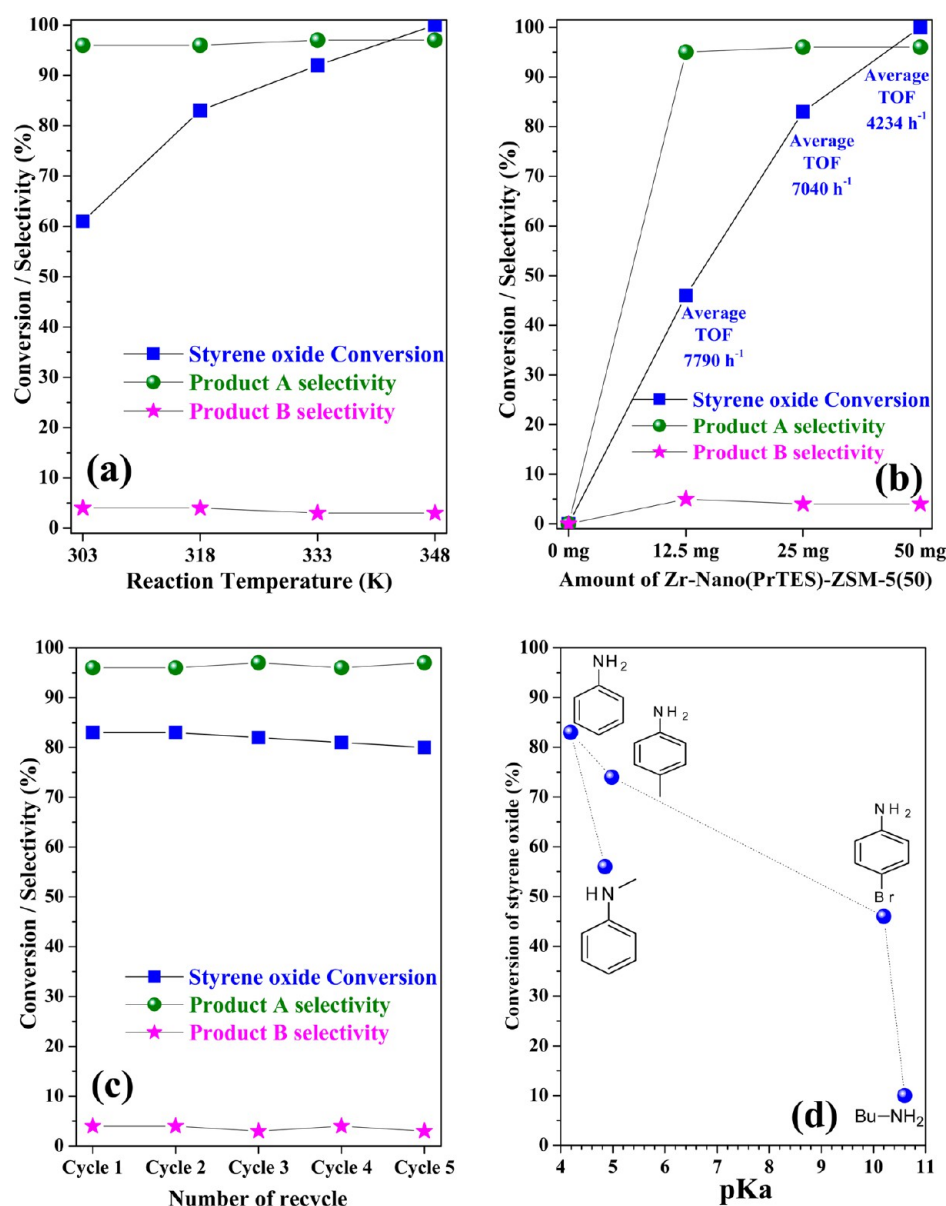


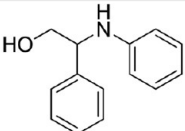
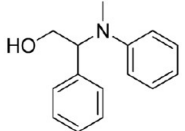
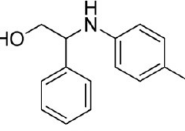
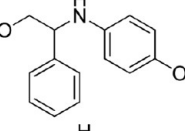
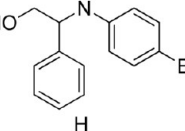
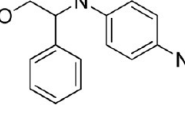
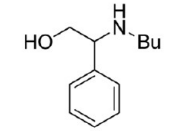
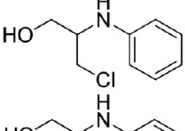
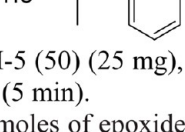
Figure 4. (a) Influence of reaction temperature [catalyst = 25 mg, time (5 min)], (b) influence of catalyst amount [temperature = 318 K, time = 5 min], (c) catalytic activity data during the recycling experiment [catalyst amount = 25 mg, temperature = 318 K, time = 5 min], and (d) correlation between catalytic activity and pK_a of amines in the ring-opening reaction of styrene oxide (5 mmol) with aniline (5 mmol) over Zr-Nano(PrTES)-ZSM-5 (50).

oxide was investigated using Zr-Nano(PrTES)-ZSM-5 (50) (Figure 4a). As the temperature increased from 303 K to 348 K, the conversion of styrene oxide increased from 61 mol % to 100 mol % (average TOF values of 4476–7337 h⁻¹). It is interesting to note that, unlike the conventional process, the ring opening of styrene oxide occurs even under ambient conditions (303 K) with high yields and selectivity for product A. The amount of catalyst also influences the conversion of styrene oxide. As the catalyst amount increased, the epoxide conversion also increased (Figure 4b). When the average TOF was taken into account, for 5 mmol of styrene oxide, 25 mg of catalyst exhibited a better result than that of 50 mg of catalyst. Si/Zr molar ratio also influenced the styrene oxide conversion. Zr-Nano(PrTES)-ZSM-5 prepared with high Si/Zr exhibited higher activity (compare average TOFs of entries 7–9 in Table 2). This result confirmed that all Zr sites present in the catalyst (prepared with high Si/Zr) are involved in the reaction.

The catalyst was found to be stable and recyclable. Recycling experiments were conducted to establish the stability of the catalyst (Figure 4c). For the recycling study, at the end of reaction, 5 mL of dichloromethane was added and the catalyst was separated by centrifugation. Thereafter, it was washed with another 5 mL of dichloromethane, dried at 373 K for 4 h, and reused in subsequent cycles. Recycling experiments confirm that no significant change in the activity was observed, even after 5 cycles. ICP analysis confirmed that Zr was not leached during the reaction. Textural characterizations using XRD and surface area analysis confirmed that the catalyst is stable.

Having found the optimized reaction condition, applicability of Zr-Nano(PrTES)-ZSM-5 (50) was investigated in the synthesis of wide range of β -amino alcohols by varying the epoxides and amines. A range of β -amino alcohols was produced with high regioselectivity from styrene oxide and different amines (see Table 3). Compared to the substituted

Table 3. Aminolysis of Epoxides and Amines over Zr-Nano(PrTES)-ZSM-5 (50)

E. No.	Epoxide	Amine	β -amino alcohol	Epoxide Conv. (%)	β -amino alcohol Sel. (%)	Average TOF (h^{-1})
1	Styrene oxide	Aniline		83	96	7040
2	Styrene oxide	N-methyl aniline		56	97	4196
3	Styrene oxide	<i>p</i> -Toluidine		74	98	6277
4	Styrene oxide	<i>p</i> -Amino phenol		33	97	2802
5	Styrene oxide	<i>p</i> -Bromo aniline		46	97	3905
6	Styrene oxide	<i>p</i> -Nitro aniline		27	96	2289
7	Styrene oxide	Butyl amine		5	14	424
8	Epichlorohydrine	Aniline		98	98	8309
9	Propylene oxide	Aniline		47	94	3988

Reaction conditions: Zr-Nano(PrTES)-ZSM-5 (50) (25 mg), epoxide (5 mmol), amine (5 mmol), reaction temperature (318 K), reaction time (5 min).

Average TOF (h^{-1}) = Turnover frequency [moles of epoxide converted per mole of active Zr per hour]

anilines, aniline produced high yield of the desired product A. This result confirmed that reactivity of amines also influences the styrene oxide conversion. The product yield was lower when aliphatic primary amine such as cyclohexyl amine was used instead of aniline. Very high epoxide conversion (99 mol %) and selectivity of product A (98 mol %) were obtained, when epichlorohydrin (instead of styrene oxide) was reacted with aniline (Table 3, entry 1). The reactivity (% conversion or average TOF) decreased in the following order:

epichlorohydrin > styrene oxide > propene oxide

(see Table 3). Trends in the catalytic activity can be explained based on $\text{p}K_a$ and adsorption of reactant molecules. In most of

the amine substrates, there is good correlation between $\text{p}K_a$ of amine with average TOF (Figure 4d). The rate of the reaction decreased (decrease in average TOF), when the basicity ($\text{p}K_a$) of the amine increased. For a catalyst to exhibit high catalytic activity, there should be an optimum bonding between the catalyst active sites and reactant molecules. If reactants adsorbed strongly on the active sites, then it will not be further available for the reaction; therefore, the catalytic activity will also decrease. Zirconosilicate/titanosilicate is an acid catalyst; therefore, it can interact with amine (base molecule). If amine is strongly bonded with the Zr/Ti acid sites, then the amine adsorbed sites will not be available to activate epoxide for the ring-opening reaction. As a result, the activity would be

Table 4. Competitive Adsorption of Epoxides and Aniline at Zr-Nano(PrTES)-ZSM-5 (50)

adsorbent	Amount Adsorbed (mmol/g catalyst)		relative adsorption ratio: epoxide/aniline	epoxide conversion (%) ^c	average TOF (h ⁻¹) ^d
	epoxide	aniline			
styrene oxide ^a + aniline	0.16	0.14	1.14	38	3223
epichlorohydrin ^a + aniline	0.16	0.12	1.33	51	4324
propylene oxide ^b + aniline	0.02	0.08	0.25	16	1358

^a100 mg of Zr-Nano(PrTES)-ZSM-5 (50) was suspended for 5 min in equimolar amounts (2 mmol) of epoxide and aniline dissolved in 5 mL of solvent (DCM). The catalyst, then, was separated and the concentration of the substrate in the liquid portion was determined by gas chromatography. The amount adsorbed on the catalyst surface was determined by difference. ^b100 mg of Zr-Nano(PrTES)-ZSM-5 (50) was suspended for 5 min in equimolar amounts (2 mmol) of epoxide and aniline dissolved in 5 mL of solvent (toluene). The catalyst, then, was separated and the concentration of the substrate in the liquid portion was determined by gas chromatography. The amount adsorbed on the catalyst surface was determined by difference. ^cEpoxide conversions and average TOF at 298 K after 5 min of the reaction. ^dAverage TOF (h⁻¹) = turnover frequency [moles of epoxide converted per mole of active Zr per hour].

Table 5. Comparative Catalytic Activity Data for the Aminolysis of Styrene Oxide with Aniline over Various Catalysts Reported in the Literature with the Catalysts Investigated in This Study

entry	catalyst	temperature/time	average TOF ^a (h ⁻¹)	ref
1	ZnCl ₂	308 K/6 h	7	20b
2	MnCl ₂ ·4H ₂ O	308 K/6 h	6	20b
3	sulfated mesoporous carbon (CMNS)	353 K/24 h	≪1	22
4	anhydrous AlCl ₃	308 K/6 h	7	20b
5	TiO ₂	308 K/6 h	1	20b
6	TS-1 (30)	308 K/6 h	52	20b
7	Ti-MCM-41 (30)	308 K/6 h	121	20b
8	Ti-SBA-15 (30)	308 K/6 h	109	20b
9	Ti-SBA-12 (30)	308 K/6 h	147	20b
10	Ti-SBA-16 (30)	308 K/6 h	156	20b
11	Ti-Nano(PrTES)-ZSM-5 (50)	308 K/5 min	332	this work
12	Ti-Nano(TPHAC)-ZSM-5 (50)	308 K/5 min	311	this work
13	Zr-ZSM-5 (50)	308 K/5 min	1517	this work
14	Zr-Nano(PrTES)-ZSM-5 (50)	308 K/5 min	5767	this work
14	Zr-Nano(PrTES)-ZSM-5 (100)	308 K/5 min	6481	this work

^aAverage TOF (h⁻¹) = turnover frequency [moles of epoxide converted per mole of active metal (Ti/Zr/Al) per hour].

lesser for strongly adsorbed amines such as cyclohexyl amine compared to aniline. We can conclude that preferential adsorption of epoxide over amine is an important factor for the ring-opening reaction. First epoxides are preferentially adsorbed and activated at acid sites and then this activated epoxide molecules react with amines (either adsorbed on surface or available in bulk reaction solution). To confirm our hypothesis, competitive adsorption experiments were performed in which the catalyst (100 mg) was suspended in equimolar (2 mmol) amounts of epoxide (styrene oxide, epichlorohydrin, or propylene oxide) and aniline dissolved in 5 mL of CH₂Cl₂ (Table 4). The adsorption of both epoxide and aniline were estimated and compared with the relative adsorption of various epoxides and aniline with catalytic activity (average TOF). Table 4 clearly shows that, for higher epoxide/amine adsorption ratios, higher average TOF values were obtained. Based on the adsorption experiments, pK_a values, and catalytic investigations, one can conclude that the activity is highly dependent on the preferential adsorption of epoxide and pK_a of amines. In addition to GC analysis, the progress of the reaction was monitored by ¹H NMR for aminolysis of styrene oxide with aniline (see details in the Supporting Information). A comparative catalytic data for the aminolysis reaction obtained in this study is presented, along with the published literature (Table 5), which confirms that nanocrystalline zirconosilicate investigated in this study is much more efficient than the catalysts reported in the literature.

The scope of the ring opening of epoxide was extended to the alcoholysis of epoxide for the synthesis of β-alkoxy alcohols. In principle, alcoholysis of styrene oxide should produce two products: C and D (see Scheme 1a). However, under our experimental conditions, we did not observe product D; instead, we observed another side product (E), i.e., phenyl acetaldehyde. The influence of reaction parameters such as reaction temperature (Figure 5b), amount of catalyst, Si/Zr ratio, and epoxide/alcohol ratio (Figure 5a) was investigated and the results are summarized in Table 6 and Figure 5. Study reveals that high catalytic activity was observed when epoxide/alcohol ratio was 1:30. With further increases in epoxide/alcohol ratio, only marginal improvement was observed (Figure 5a). Therefore, epoxide/alcohol ratio of 1:30 was chosen for further studies. In this manuscript, only comparative catalytic activities of alcoholysis of styrene oxide with methanol are summarized over various catalysts investigated in this study (see Table 6). Catalyst was found to be recyclable and no change in the activity was observed even after 5 recycles (Figure 5c). Similar to aminolysis reaction, in this reaction also, nanocrystalline zirconosilicate exhibited higher activity. Investigation revealed that the highest catalytic activity was observed, when methanol was chosen as alcohol. Progressive decrease in the activity was observed when chain length of the alcohol was increased (Table 7). This decrease in the catalytic activity can be correlated with the increase in the pK_a values of alcohols (Figure 5d). It may be noted that, in addition to the main

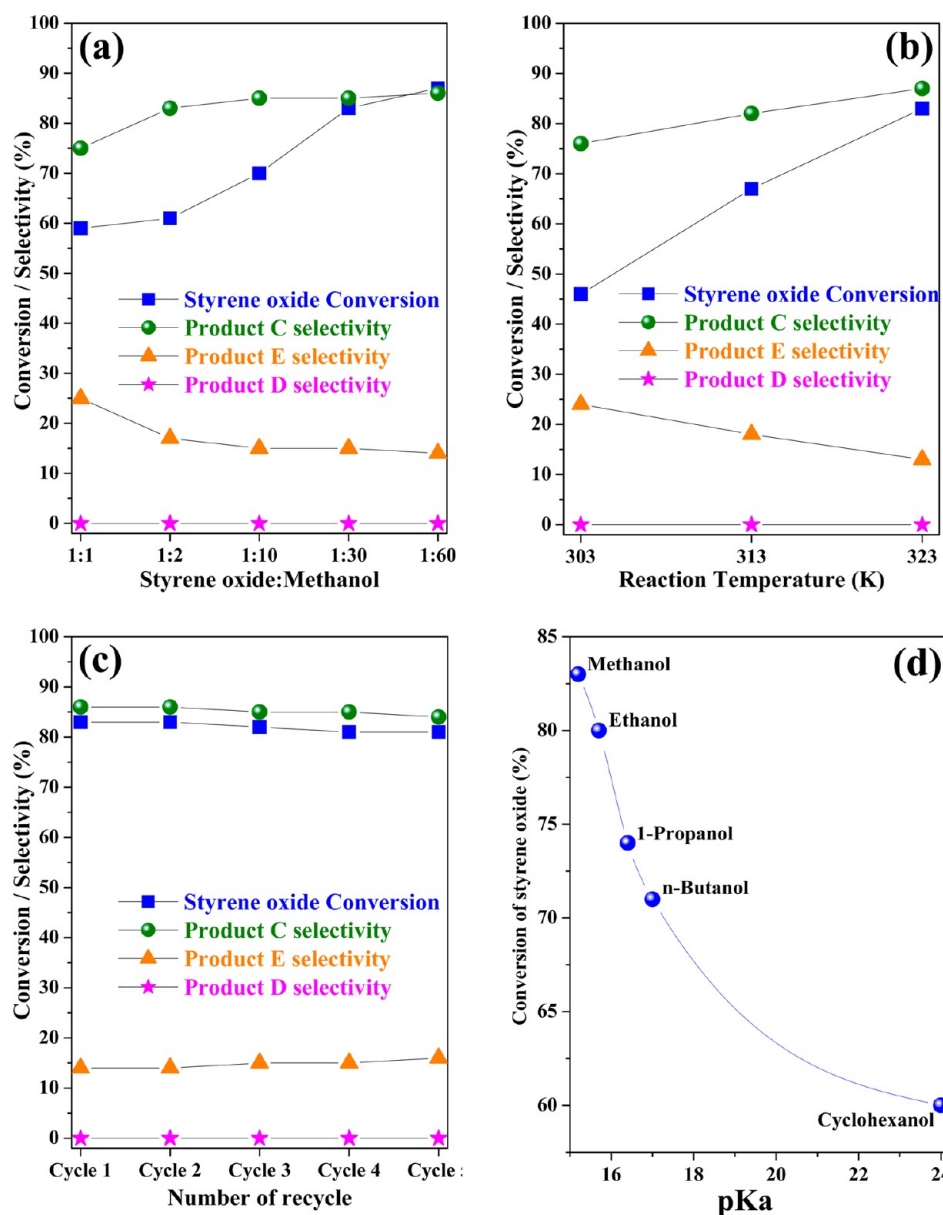


Figure 5. (a) Influence of styrene oxide (SO)/methanol (MeOH) ratio [catalyst = 25 mg, temperature = 323 K, time = 45 min], (b) influence of reaction temperature [catalyst = 25 mg, SO:MeOH ratio = 1:30 (mmol/mmol), time = 45 min], (c) catalytic activity data during recycling experiment [catalyst = 25 mg, SO:MeOH ratio = 1:30 (mmol/mmol), temperature = 323 K, time = 45 min], (d) correlation between catalytic activity and pK_a of alcohols in the ring-opening reaction of SO (1 mmol) with alcohols (30 mmol) over Zr-Nano(PrTES)-ZSM-5 (50).

Table 6. Alcoholysis of Styrene Oxide with Methanol over Various Zeolite Catalysts^a

entry	catalyst	styrene oxide conversion (%)	product (C/E) selectivity ^b (%)	average TOF ^c (h ⁻¹)
1	none	0		
2	Al-ZSM-5 (50)	16	35/65	27
3	Ti-ZSM-5 (50)	9	30/70	17
4	Zr-ZSM-5 (50)	27	71/29	54
5	Ti-Nano(PrTES)-ZSM-5 (50)	20	58/42	39
6	Ti-Nano(TPHAC)-ZSM-5 (50)	21	52/48	58
7	Zr-Nano(PrTES)-ZSM-5 (30)	89	86/14	117
8	Zr-Nano(PrTES)-ZSM-5 (50)	83	87/13	157
9	Zr-Nano(PrTES)-ZSM-5 (100)	65	86/14	229
10	Zr-Nano(TPHAC)-ZSM-5 (50)	75	85/15	142

^aReaction conditions: catalyst (25 mg), styrene oxide (1 mmol), methanol (30 mmol), reaction temperature (323 K), reaction time (45 min.). ^b[C] = 2-methoxy-2-phenylethanol. [E] = phenyl acetaldehyde. ^cAverage TOF (h⁻¹) = turnover frequency [moles of epoxide converted per mole of active metal (Ti/Zr/Al) per hour]

Table 7. Alcoholysis of Styrene Oxide with Alcohols over Zr-Nano(PrTES)-ZSM-5 (50)

Entry No.	Nucleophile	β -Alkoxy alcohol	Styrene oxide Conv. (%)	β -Alkoxy alcohol Sel. (%)	Average TOF (h^{-1})
1	Methanol		83	87	157
2	Ethanol		80	85	151
3	1-Propanol		74	84	140
4	1-Butanol		71	84	134
5	Cyclohexanol		60	80	113

Reaction conditions: Zr-Nano(PrTES)-ZSM-5 (50) (25 mg), styrene oxide (1 mmol), alcohol (30 mmol), reaction temperature (323 K), reaction time (45 min.)

Average TOF (h^{-1}) = Turnover frequency [moles of epoxide converted per mole of active Zr per hour]

Table 8. Hydroamination of Methyl Acrylate with Aniline over Different Zeolite Catalysts^a

entry	catalyst	aniline conversion (%)	product [F] selectivity ^b (%)	average TOF ^c (h^{-1})
1	none			
2	Al-ZSM-5 (50)	5	99	0.5
3	Ti-ZSM-5 (50)	29	98	6
4	Zr-ZSM-5 (50)	42	97	10
5	Ti-Nano(PrTES)-ZSM-5 (50)	44	97	10
6	Ti-Nano(TPHAC)-ZSM-5 (50)	44	96	10
7	Zr-Nano(PrTES)-ZSM-5 (30)	99	98	15
8	Zr-Nano(PrTES)-ZSM-5 (50)	95	97	22
9	Zr-Nano(PrTES)-ZSM-5 (100)	72	97	29
10	Zr-Nano(TPHAC)-ZSM-5 (50)	94	97	22

^aReaction conditions: catalyst (25 mg), methyl acrylate (2.1 mmol), aniline (2 mmol), reaction temperature (353 K), reaction time (12 h). ^bProduct [F] = *N*-[2-(methoxycarbonyl) ethyl]aniline. ^cAverage TOF (h^{-1}) = turnover frequency [moles of epoxide converted per mole of active metal (Ti/Zr/Al) per hour].

product, one side product was also observed during the alcoholysis reaction of styrene oxide. Zr incorporation favors the formation of the main product. More amount of side product was formed in microcrystalline ZSM-5 when compared to nanocrystalline ZSM-5 materials. High external surface area and intercrystalline mesopores both enhance the accessibility of reactant molecules and, therefore, the formation of side product is reduced. The mechanism (described by Scheme S1 in the Supporting Information) shows that the side product is formed directly from styrene oxide, which confirms that microporous zeolites can interact only to styrene oxide due to preferential adsorption of styrene oxide and pore diffusion limitation. To confirm this hypothesis, two experiments were carried out. First experiment was based on the competitive adsorption of styrene oxide and methanol on Al-ZSM-5 (50) and Zr-Nano(PrTES)-ZSM-5 (50) (see Table S3 in the Supporting Information). Second experiment was to evaluate the catalytic activity of Al-

ZSM-5 (50) and Zr-Nano(PrTES)-ZSM-5 (50) by taking styrene oxide as only reactant molecule (see Table S4 in the Supporting Information). Competitive adsorption experiment reveals that styrene oxide adsorption was more compared to methanol in both the catalysts, especially in Al-ZSM-5 (50), which is responsible for the formation of more side product. The second experiment reveals that side product is formed in higher amounts when no methanol was added in the reaction mixture. In addition to the side product, 1-phenylethane-1,2-diol was also formed. To confirm the origin of 1-phenylethane-1,2-diol, one additional experiment was performed, wherein styrene oxide was reacted with H₂O using Zr-Nano(PrTES)-ZSM-5 (50), which leads to the formation of product E and 1-phenylethane-1,2-diol. In addition to GC analysis, the progress of the reaction was monitored by ¹H NMR for alcoholysis of styrene oxide with methanol (see details in the Supporting Information).

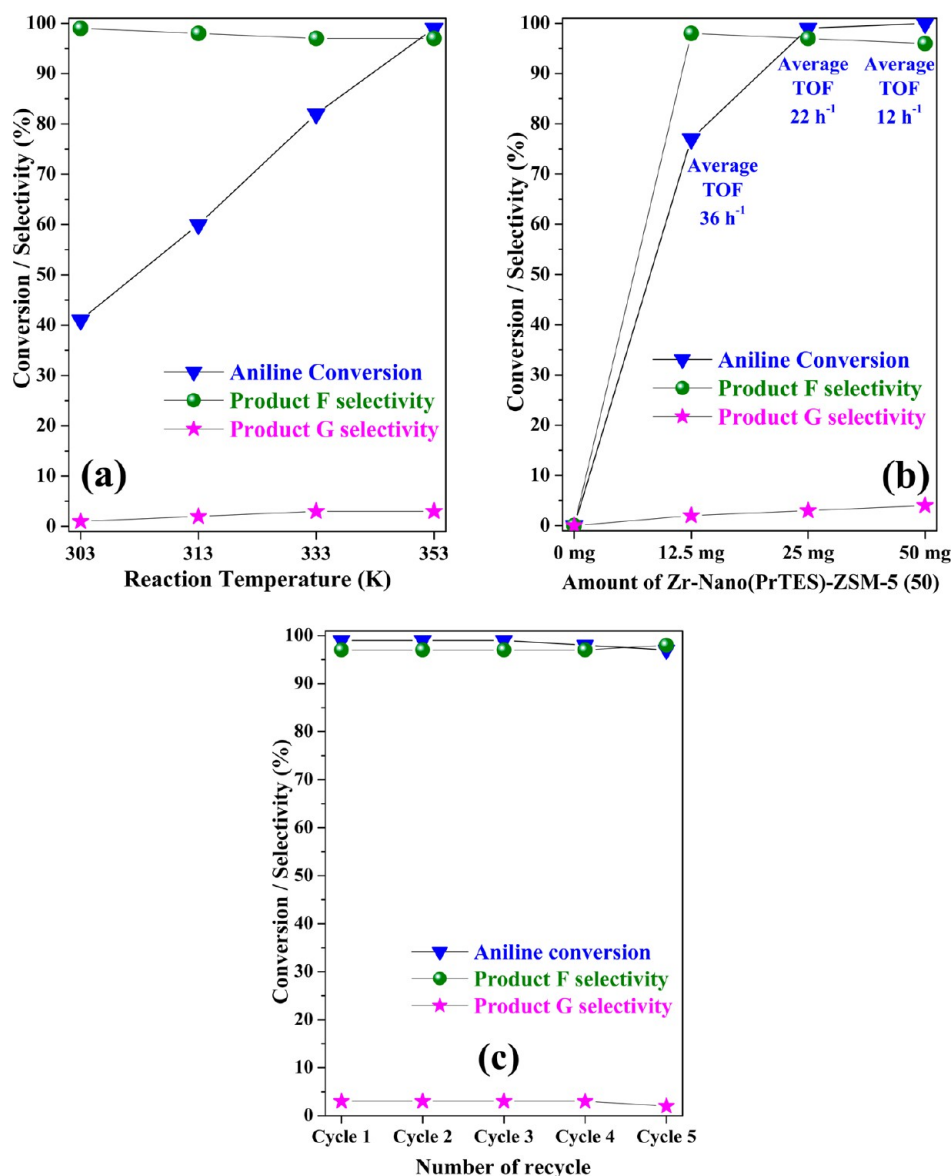


Figure 6. (a) Influence of reaction temperature [catalyst = 25 mg, time (12 h)], (b) influence of catalyst amount [temperature = 353 K, time = 12 h], and (c) catalytic activity data during recycling experiment [catalyst = 25 mg, temperature = 353 K, time = 12 h] in the hydroamination reaction of methyl acrylate (2.1 mmol) with aniline (2 mmol) over Zr-Nano(PrTES)-ZSM-5 (50) with time = 12 h.

3.2.2. Hydroamination Reaction. Activity of nanocrystalline ZSM-5 materials was investigated in the hydroamination of methyl acrylate with aniline. Zeolites catalyzed the reaction to give mainly anti-Markovnikov adduct, *N*-[2-(methoxycarbonyl)ethyl]aniline (F), and no Markovnikov adduct: *N*-[1-(methoxycarbonyl)ethyl]aniline was detected. In addition to main product (F); *N,N'*-bis[2-(methoxycarbonyl)ethyl]aniline (G) was detected as a side product. The side product G was formed by the double addition of methyl acrylate to aniline (Scheme 1b). Table 8 summarizes the catalytic activities for the hydroamination of methyl acrylate with aniline over zeolite catalysts investigated in this study. The order of the activity in the case of conventional microporous ZSM-5 materials investigated in this study is

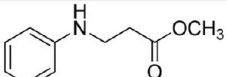
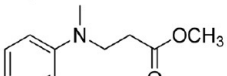
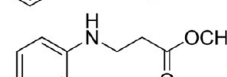
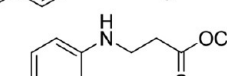

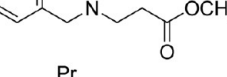
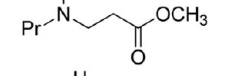


which confirmed that Zr incorporation in the framework also is ideally suited for the hydroamination reaction. Activity of nanocrystalline zirconosilicate exhibited the highest activity. ¹H

NMR spectra of pure product F and reaction mixture (for the reaction of methyl acrylate and aniline) are shown in Figure S8 in the Supporting Information.

Influence of reaction parameters were optimized using Zr-Nano(PrTES)-ZSM-5 (50). Figure 6a shows the influence of reaction temperature on catalytic activity and the selectivity of product F over Zr-Nano(PrTES)-ZSM-5 (50). The activity was strongly affected by the increase of the temperature, and the conversion of aniline almost linearly increased with the temperature up to 353 K. It may further be noted that a marginal increase in the side product selectivity was observed upon increasing the reaction temperature. Effect of the catalyst amount on the hydroamination of methyl acrylate with aniline over Zr-Nano(PrTES)-ZSM-5 (50) is shown in Figure 6b. It seems that 25 mg of the catalyst for 2 mmol of aniline is an optimal amount to achieve the higher activity. Increasing the amount of the catalyst up to 50 mg resulted only in marginal increase in the product yield. Si/Zr molar ratio influenced the aniline conversion. Zr-Nano(PrTES)-ZSM-5 samples prepared

Table 9. Hydroamination of Methyl Acrylate with Amines over Zr-Nano(PrTES)-ZSM-5 (50)

Entry No.	Amine	Product	Time (h)	Amine Conv. (%)	Product Sel. (%)	Average TOF (h ⁻¹)
1	Aniline		12	99	97	22
2	N-methylaniline		12	77	99	17
3	p-Toluidine		12	95	99	21
4	4-Bromo aniline		12	73	98	16
5	Benzyl amine		0.5	83	99	468
6	dipropylamine		0.5	62	100	350
7	Cyclohexylamine		0.5	94	100	527

Reaction conditions: Zr-Nano(PrTES)-ZSM-5 (50) (25mg), methyl acrylate (2.1mmol), amine (2 mmol), reaction temperature (353 K).

Average TOF (h⁻¹) = Turnover frequency [moles of epoxide converted per mole of active Zr per hour]

with high Si/Zr exhibited higher activity (Compare average TOFs of entries 7–9 in Table 8.) Recycling experiments confirmed that no significant change in the activity was observed even after 5 recycles (Figure 6c). ICP analysis confirmed that Zr was not leached during the reaction. Textural characterizations using XRD and surface area analysis confirmed that the catalyst is stable.

In contrast to aminolysis, activation of amine is an important step in hydroamination reaction (see Scheme S2 in the Supporting Information). The amine is activated on the acidic sites in the first step, aniline is adsorbed to the acid site of zeolite (X) to form ammonium cation (Y) by acid base interaction, followed by Michael addition of methyl acrylate to give the monoalanine ammonium intermediate (Z). The intermediate (Z), then, releases the anti-Markovnikov adduct F to regenerate acid site of catalyst (X). Further addition of methyl acrylate to the intermediate (Z) affords side product with regeneration of active catalyst acid site. Let us assume that methyl acrylate is adsorbed at the acid site of zeolite catalyst, which is followed by the formation of corresponding cation. In this mechanism, unfortunately, nucleophilic attack of aniline occurs preferentially to the α -carbon of methyl acrylate to give the Markovnikov adduct. But this second possibility is ruled out in our study, because no Markovnikov adduct is formed. Therefore, since our catalyst is an acid catalyst, the adsorption of aniline to acid sites of zeolite by acid–base interaction is more appropriate than that of methyl acrylate to yield the acrylate cation. Competitive adsorption of methyl acrylate and aniline over Zr-Nano(PrTES)-ZSM-5 (50) and Al-ZSM-5 (50) confirmed that amines are preferentially adsorbed on Zr-

Nano(PrTES)-ZSM-5 (50), resulting in its high activity (see Table S5 in the Supporting Information). Michael addition is also responsible for the preferential formation of anti-Markovnikov adduct. The selective formation of anti-Markovnikov adducts in the hydroamination of methyl acrylate for the formation of the intermediate “Z” is the key step for the hydroamination. Having found the optimized reaction condition, applicability of Zr-Nano(PrTES)-ZSM-5 (50) was investigated in the synthesis of wide range of amino acid derivative by varying the amines (Table 9). Reaction was more facile when aliphatic amines were reacted when compared to aromatic amines (Table 9). Significantly high catalytic activity in the case of aliphatic amines (for example, cyclohexyl amine) is well supported by the competitive adsorption experiment (see Table S5 in the Supporting Information).

Catalytic activity data in the hydroamination reaction and ring opening of epoxide with amine/alcohol suggest that isomorphous substitution of Zr in the MFI framework is responsible for the high activity. Acidity measurements confirmed that zeolites with high acidity are not suitable for these reactions. When acidity and activity are taken into the consideration for Ti-incorporated ZSM-5 materials and Zr-incorporated ZSM-5 materials, one can conclude that fine-tuning in acidity by incorporating suitable metal ion in the MFI-framework is required for these reactions. It seems that Zr incorporation provides optimum acidity for these reactions. In the case of alcoholysis/aminolysis, the Zr/Ti sites activate the epoxide. Because of the larger ionic radius (0.73 Å for Zr⁴⁺ and 0.56 Å for Ti⁴⁺) and the larger electronegative difference between M⁴⁺ and oxygen attached to epoxide ring (2.11 and 1.9

for O–Zr and O–Ti, respectively), zirconosilicates can polarize the O–Zr bond more efficiently than titanosilicates. This high polarizability of zirconosilicates is responsible for the weakening of O–C bond (of epoxide ring) and facile reaction of amine to epoxide to form desired product. Based on catalytic activity, acidity measurements, adsorption experiments, and textural properties, one can conclude that the optimum Zr polarizability, acidity, high external surface area, and intercrystalline mesopores are responsible for such a high activity of Zr-Nano(PrTES)-ZSM-5. Therefore, it can be concluded that, by fine-tuning the textural and acidic properties, it is possible to develop highly efficient catalytic materials for a particular type of reaction.

4. CONCLUSION

Nanocrystalline zirconosilicates and titanosilicates prepared using organosilane exhibited high external surface area, mesopore volume, and possess intercrystalline mesopores. Nanocrystalline zirconosilicate exhibited exceptionally high catalytic activity compared to catalysts reported in the literature for the ring opening of epoxide with nitrogen (amines)-containing and oxygen (alcohols)-containing nucleophiles and hydroamination reactions. Isomorphous substitution of Zr in zeolite framework, large surface area, and intercrystalline mesoporosity are responsible for the high catalytic activity of nanocrystalline zirconosilicate. Excellent recyclability, simplified experimental procedure, and mild conditions are some of the attractive key features for the industrial exploitation. Based on catalytic activity, acidity measurements, adsorption experiments, and textural properties, it can be concluded that optimum Zr polarizability, acidity, large external surface area, and intercrystalline mesoporosity are responsible for high activity of nanocrystalline zirconosilicates.

■ ASSOCIATED CONTENT

Supporting Information

Additional experimental details, material characterization techniques, and results and discussion as noted in text. This material is available free of charge via the Internet at <http://pubs.acs.org>.

■ AUTHOR INFORMATION

Corresponding Author

*Tel.: +91-1881-242175. Fax: +91-1881-223395. E-mail address: rajendra@iitrpr.ac.in.

Notes

The authors declare no competing financial interest.

■ ACKNOWLEDGMENTS

Authors are thankful to DST for financial assistance through DST Project No. SB/S1/PC-91/2012. R.K. is grateful to CSIR, New Delhi for the SRF fellowship. We acknowledge the Director of IIT Ropar for constant encouragements.

■ REFERENCES

- (1) (a) Corma, A. *Chem. Rev.* **1995**, *95*, 559–614. (b) Okuhara, T.; Mizuno, N.; Misono, M. *Adv. Catal.* **1996**, *41*, 113–252.
- (2) Torborg, C.; Beller, M. *Adv. Syn. Catal.* **2009**, *351*, 3027–3043.
- (3) Sartori, G.; Ballini, R.; Bigi, F.; Bosica, G.; Maggi, R.; Righi, P. *Chem. Rev.* **2004**, *104*, 199–250.
- (4) (a) Davis, M. E. *Nature* **2002**, *417*, 813–821. (b) Wilson, K.; Clark, J. H. *Pure Appl. Chem.* **2000**, *72*, 1313–1319. (c) Thomas, J. M. *Angew. Chem., Int. Ed.* **1988**, *27*, 1673–1691.
- (5) (a) Schüth, F.; Schmidt, W. *Adv. Mater.* **2002**, *14*, 629–638. (b) Cundy, C. S.; Cox, P. A. *Chem. Rev.* **2003**, *103*, 663–701.
- (6) (a) Kresge, C. T.; Leonowicz, M. E.; Roth, W. J.; Vartuli, J. C.; Beck, J. S. *Nature* **1992**, *359*, 710–712. (b) Tanev, P. T.; Pinnavaia, T. J. *Science* **1995**, *267*, 865–867. (c) Kim, T. W.; Kleitz, F.; Paul, B.; Ryoo, R. J. *Am. Chem. Soc.* **2005**, *127*, 7601–7610.
- (7) (a) Tao, Y.; Kanoh, H.; Abrams, L.; Kaneko, K. *Chem. Rev.* **2006**, *106*, 896–910. (b) Pérez-Ramírez, J.; Christensen, C. H.; Egeblad, K.; Christensen, C. H.; Groen, J. C. *Chem. Soc. Rev.* **2008**, *37*, 2530–2542.
- (8) (a) Holland, B. T.; Abrams, L.; Stein, A. J. *Am. Chem. Soc.* **1999**, *121*, 4308–4309. (b) Jacobsen, C. J. H.; Madsen, C.; Houzvicka, J.; Schmidt, I.; Carlsson, A. J. *Am. Chem. Soc.* **2000**, *122*, 7116–7117. (c) Egeblad, K.; Christensen, C. H.; Kustova, M.; Christensen, C. H. *Chem. Mater.* **2008**, *20*, 946–960. (d) Srivastava, R.; Iwasa, N.; Fujita, S. i.; Arai, M. *Chem.—Eur. J.* **2008**, *14*, 9507–9511. (e) Wang, R.; Liu, W.; Ding, S.; Zhang, Z.; Li, J.; Qiu, S. *Chem. Commun.* **2010**, *46*, 7418–7420.
- (9) Srivastava, R.; Choi, M.; Ryoo, R. *Chem. Commun.* **2006**, 4489–4491.
- (10) (a) Na, K.; Jo, C.; Kim, J.; Ahn, W. S.; Ryoo, R. *ACS Catal.* **2011**, *1*, 901–907. (b) Sashkina, K.; Labko, V.; Rudina, N.; Parmon, V.; Parkhomchuk, E. J. *Catal.* **2013**, *299*, 44–52.
- (11) (a) Kore, R.; Satpati, B.; Srivastava, R. *Chem.—Eur. J.* **2011**, *17*, 14360–14365. (b) Kore, R.; Sridharkrishna, R.; Srivastava, R. *RSC Adv.* **2013**, *3*, 1317–1322. (c) Kore, R.; Srivastava, R. *RSC Adv.* **2012**, *2*, 10072–10084. (d) Kore, R.; Srivastava, R. *Catal. Commun.* **2012**, *18*, 11–15. (e) Kore, R.; Tamma, M.; Srivastava, R. *Catal. Today* **2012**, *198*, 189–196. (f) Kaur, B.; Prathap, M. U. A.; Srivastava, R. *ChemPlusChem* **2012**, *77*, 1119–1127.
- (12) (a) Zhou, J.; Hua, Z.; Cui, X.; Ye, Z.; Cui, F.; Shi, J. *Chem. Commun.* **2010**, *46*, 4994–4996. (b) Koekkoek, A.; Kim, W.; Degimenci, V.; Xin, H.; Ryoo, R.; Hensen, E. J. *Catal.* **2013**, *299*, 81–89. (c) Zhao, Z.; Liu, Y.; Wu, H.; Li, X.; He, M.; Wu, P. J. *Porous Mater.* **2010**, *17*, 399–408. (d) Cheneviere, Y.; Chieux, F.; Caps, V.; Tuel, A. J. *Catal.* **2010**, *269*, 161–168.
- (13) (a) Chen, L.-H.; Xu, S.-T.; Li, X.-Y.; Tian, G.; Li, Y.; Rooke, J. C.; Zhu, G.-S.; Qiu, S.-L.; Wei, Y.-X.; Yang, X.-Y. *J. Colloid Interface Sci.* **2012**, *377*, 368–374. (b) Zhao, Z.; Liu, Y.; Wu, H.; Li, X.; He, M.; Wu, P. *Microporous Mesoporous Mater.* **2009**, *123*, 324–330.
- (14) (a) Ager, D. J.; Prakash, I.; Schaad, D. R. *Chem. Rev.* **1996**, *96*, 835–875. (b) Bergmeier, S. C. *Tetrahedron* **2000**, *56*, 2561–2576. (c) Corey, E. J.; Zhang, F. Y. *Angew. Chem., Int. Ed.* **1999**, *38*, 1931–1934. (d) O'Brien, P. *Angew. Chem., Int. Ed.* **1999**, *38*, 326–329.
- (15) Baylon, C.; Prestat, G.; Heck, M.-P.; Mioskowski, C. *Tetrahedron Lett.* **2000**, *41*, 3833–3835.
- (16) Müller, T. E.; Beller, M. *Chem. Rev.* **1998**, *98*, 675–703.
- (17) Juaristi, E.; López-Ruiz, H. *Curr. Med. Chem.* **1999**, *6*, 983–1004.
- (18) (a) Procopio, A.; Gaspari, M.; Nardi, M.; Oliverio, M.; Rosati, O. *Tetrahedron Lett.* **2008**, *49*, 2289–2293. (b) Malhotra, S. V.; Andral, R. P.; Kumar, V. *Syn. Commun.* **2008**, *38*, 4160–4169. (c) Bhanushali, M. J.; Nandurkar, N. S.; Bhor, M. D.; Bhanage, B. M. *Tetrahedron Lett.* **2008**, *49*, 3672–3676. (d) Moghadam, M.; Tangestaninejad, S.; Mirkhani, V.; Mohammadpoor-Baltork, I.; Gorjipoor, S.; Yazdani, P. *Syn. Commun.* **2009**, *39*, 552–561.
- (19) (a) Vijender, M.; Kishore, P.; Narender, P.; Satyanarayana, B. J. *Mol. Catal. A: Chem.* **2007**, *266*, 290–293. (b) Kureshy, R. I.; Singh, S.; Khan, N. u. H.; Abdi, S. H. R.; Suresh, E.; Jasra, R. V. *J. Mol. Catal. A: Chem.* **2007**, *264*, 162–169. (c) Robinson, M. W. C.; Timms, D. A.; Williams, S. M.; Graham, A. E. *Tetrahedron Lett.* **2007**, *48*, 6249–6251. (d) Chakravarti, R.; Oveisi, H.; Kalita, P.; Pal, R. R.; Halligudi, S. B.; Kantam, M. L.; Vinu, A. *Microporous Mesoporous Mater.* **2009**, *123*, 338–344. (e) Satyarathi, J. K.; Saikia, L.; Srinivas, D.; Ratnasamy, P. *Appl. Catal., A* **2007**, *330*, 145–151.
- (20) (a) Saikia, L.; Satyarathi, J. K.; Srinivas, D.; Ratnasamy, P. *J. Catal.* **2007**, *252*, 148–160. (b) Kumar, A.; Srinivas, D. *J. Catal.* **2012**, *293*, 126–140.
- (21) Shannon, R. *Acta Crystallogr. Sect. A: Cryst. Phys., Diffr., Theor. Gen.* **1976**, *32*, 751–767.

(22) Matos, I.; Neves, P. D.; Castanheiro, J. E.; Perez-Mayoral, E.; Martin-Aranda, R.; Duran-Valle, C.; Vital, J.; Botelho Do Rego, A. M.; Fonseca, I. M. *Appl. Catal., A* **2012**, *439–440*, 24–30.